



Predicting Pacific cod thermal spawning habitat in a changing climate

J. S. Bigman^{1,*}, B. J. Laurel², K. Kearney³, A. J. Hermann^{3,4}, W. Cheng^{3,4}, K. K. Holsman⁵, and L. A. Rogers¹

¹Recruitment Processes Program, Alaska Fisheries Science Center, NOAA Fisheries, Seattle, WA, 98115, USA

²Fisheries Behavioral Ecology Program, Alaska Fisheries Science Center, NOAA Fisheries, Newport, OR, 97365, USA

³Cooperative Institute for Climate, Ocean, and Ecosystem Studies, University of Washington, Seattle, WA, 98195, USA

⁴Ocean Environment Research Division, NOAA/Pacific Marine Environmental Laboratory, Seattle, WA, 98115, USA

⁵Resource Ecology and Fisheries Management Division, Alaska Fisheries Science Center, NOAA Fisheries, Seattle, WA, 98115, USA

*Corresponding author: tel/fax: +1 (206) 698-7372; e-mail: jennifersbigman@gmail.com.

Warming temperatures elicit shifts in habitat use and geographic distributions of fishes, with uneven effects across life stages. Spawners and embryos often have narrower thermal tolerances than other life stages, and are thus particularly sensitive to warming. Here, we examine the spatiotemporal variability of thermal spawning habitat for Pacific cod in the eastern Bering Sea. Specifically, we use bottom temperatures from downscaled global climate models coupled with an experimentally-derived hatch success and temperature relationship to predict how the spatial extent, mean latitude, and consistency of thermal spawning habitat has varied over time. Predictions are validated with observations of spawning adults and early larvae. We find that habitat availability has not increased in the past but is predicted to increase and shift northward in the future, particularly if no climate change mitigation occurs. Habitat hotspots are consistent across shorter time periods but do shift across the shelf by the end of the century such that highly suitable areas in the past and present are not predicted to be suitable in the future. This work highlights the importance of coupling experimental data with climate models to identify the complex and mechanistic dynamics among temperature, life histories, and ecology, particularly under climate change.

Keywords: biogeography, earth systems models, gadids, spawning dynamics, species distribution models.

Introduction

Changing environmental conditions have elicited changes in the ecology, physiology, and life histories of marine fish (Parmesan and Yohe, 2003; Poloczanska *et al.*, 2013). One of the most notable, widespread responses to environmental change is shifts in patterns of habitat use and geographic distributions (Pinsky *et al.*, 2013; Burrows *et al.*, 2014). These include changes in seasonal use of habitat, poleward distributional shifts, and movement of species into deeper waters (Dulvy *et al.*, 2008; Fossheim *et al.*, 2015). Although such distributional shifts are likely related to a host of factors, few are as relevant across species and systems as temperature. Changes in temperature have been linked to changes in habitat use and distribution across scales, ranging from individuals tracking preferred temperatures to the large-scale, global redistribution of populations and species (Pörtner and Farrell, 2008; Fredston *et al.*, 2021). Indeed, thermal limits and tolerance ranges—the range of temperatures a species can physiologically withstand—are thought to shape species distributions and set range boundaries now and in the future (Sunday *et al.*, 2019; Pörtner, 2021).

The effect of temperature on organismal physiology is not static across an individual's lifespan and, thus, thermal limits and tolerance typically change with size and ontogeny (Dahlke *et al.*, 2020). These changes in thermal sensitivities translate into uneven shifts in habitat use and distribution across life stages (Barbeaux and Hollowed, 2018; Cote *et al.*, 2021).

In particular, spawners and developing embryos are thought to exhibit the narrowest thermal tolerances, resulting in a tight relationship between spawning habitat (the realized location and its characteristics where fish spawn) and temperature (Dahlke *et al.*, 2018, 2020; Pörtner, 2021). For example, reductions in the amount of thermally-suitable spawning habitat (locations suitable for spawning based on embryo thermal tolerance) due to warming disproportionately affect Nassau Grouper (*Epinephelus striatus*) spawners, whose thermal range is narrower than that of nonspawners (Asch and Erisman, 2018). Additionally, compared to other life stages, eggs typically occupy the least amount of habitat area (lowest habitat extent) and have the highest habitat consistency (same locations) over time (Ciannelli *et al.*, 2015, 2021). In turn, these narrow thermal preferences of spawners and embryos collectively result in spatial or temporal (or both) constraints on spawning habitat, which encompasses the habitat of both eggs and spawners (Rijnsdorp *et al.*, 2009; Ciannelli *et al.*, 2021). Thus, spawning habitat has been suggested not only to underlie reproductive potential but also may act as a “thermal bottleneck” that determines species’ vulnerability to a changing climate (Dahlke *et al.*, 2020; Ciannelli *et al.*, 2021).

Temperature-driven distributional shifts are linked to changes in population dynamics and fisheries productivity, ecosystem dynamics (e.g., species interactions), and socioeconomic aspects such as increased fishing effort and altered management practices (Rogers *et al.*, 2019). Such changes may impact spawning habitat by influencing the locations of either

Received: 13 January 2023; Revised: 4 April 2023; Accepted: 8 May 2023

Published by Oxford University Press on behalf of International Council for the Exploration of the Sea 2023. This work is written by (a) US Government employee(s) and is in the public domain in the US.

adult spawners or developing embryos. For example, a reduction in the area or temporal window for successful spawning is correlated with reduced recruitment and stock reproductive potential, as well as altered stock-recruitment dynamics (Hayes *et al.*, 1996; Dodson *et al.*, 2019; Laurel and Rogers, 2020). Additionally, changes in spawning habitat will likely affect the location and movement of adult fish, which in turn, can determine catchability in fisheries monitoring surveys, as well as fishing opportunities, as fishers often have limitations on where, when, and how they can fish (Haynie and Pfeiffer, 2013; Rogers *et al.*, 2019). Thus, understanding and predicting how spawning habitat changes with temperature and whether this confers changes in population and ecosystem dynamics can help us mitigate the effects of climate change on the livelihoods and economies fishing supports.

The Bering Sea supports some of the largest fisheries in the world yet is undergoing rapid environmental change (Fissel *et al.*, 2019; Stabeno and Bell, 2019). In particular, the dynamics of sea ice play a major role in this system, as the timing and extent of seasonal ice affect many other physical and biological factors. A region of cold ($<2^{\circ}\text{C}$) bottom water on the Bering Sea shelf—the cold pool—is formed during the freezing and melting of seasonal sea ice, and years in which there is a high areal ice extent are associated with a large cold pool (Stabeno *et al.*, 2012). The cold pool is thought to act as a barrier between arctic and subarctic communities and drive patterns of distribution and habitat use of fishes in the region (Mueter and Litzow, 2008; Stevenson and Lauth, 2019). For example, many species avoid the cold pool and thus shift their seasonal distributions depending on its location and extent (Mueter and Litzow, 2008; Stevenson and Lauth, 2019). Recent years have seen a reduction in the extent and duration of sea ice and a concomitant shrinking (or disappearance) of the cold pool, which is thought to underlie the recent northward shifts of many species in the region (Mueter and Litzow, 2008; Stabeno and Bell, 2019; Stevenson and Lauth, 2019). However, it remains unclear whether individuals' and species' responses to changes in temperature are transitory or whether redistributions are occurring on longer time scales.

Pacific cod, *Gadus macrocephalus*, is one of the economically important fish species that has been observed to expand their summer distribution from the southeastern Bering Sea into the northern Bering Sea following an extensive and protracted marine heatwave and associated loss of sea ice in the region (Stevenson and Lauth, 2019). While generally little is known about Pacific cod spawning in the Bering Sea, this species spawns in the winter in the eastern Bering Sea along the outer shelf break (around the 180 m isobath) near Zhemchug Canyon and the Pribilof Islands, and along the Aleutian Islands, particularly around Unimak Island (Figure 1; Neidetcher *et al.*, 2014; Rand *et al.*, 2014). Although Pacific cod (like many groundfish species in the region) have been observed in the northern Bering Sea seasonally in summer monitoring surveys, it is unknown whether this area is currently or will become thermally suitable for spawning. Compared to other gadids (e.g., Polar cod *Boreogadus saida*, Saffron cod *Eleginops gracilis*, and Walleye pollock *Gadus chalcogrammus*), the spawning dynamics of Pacific cod are particularly sensitive to temperature as embryos have a narrow thermal range for successful development and hatching (Figure 2; Alderdice and Forrester, 1971; Bian *et al.*, 2014, 2016; Dahlke *et al.*, 2018; Laurel and Rogers, 2020; Cote *et al.*, 2021). Such a response to temperature for Pacific cod embryos has been

shown across multiple geographic regions (Strait of Georgia: Alderdice and Forrester, 1971; Japan: Bian *et al.*, 2014, 2016; Gulf of Alaska; Laurel and Rogers, 2020). More broadly, embryo thermal tolerances for marine fish typically follow a Gaussian or Cauchy distribution, where hatch success is highest across a narrow range of temperatures (Tsoukali *et al.*, 2016). In the Gulf of Alaska, the closest location where a relationship exists for Pacific cod, hatch success increases steeply around 3°C and drops around 7°C , with the highest success around 5°C (Laurel and Rogers, 2020). Because Pacific cod lay demersal eggs that adhere to the bottom for the duration of development, their spawning dynamics are closely tied to bottom temperature (Alderdice and Forrester, 1971). Recent work in the Gulf of Alaska has shown that this narrow thermal tolerance of egg survival reduced the availability of thermally-suitable spawning habitat, which may have contributed to the stark decline in pre-recruit abundance and stock reproductive potential for this species following the marine heatwave in 2014–2016 (Laurel and Rogers, 2020). However, in the comparatively colder waters of the Bering Sea, it is unknown whether and when changes in bottom temperature may affect cod populations through potential shifts in thermally-suitable spawning habitats.

Here, we quantify how environmental temperature affects the availability of thermally-suitable spawning habitat across space and time and how this may relate to changes in fisheries productivity for Pacific cod in the eastern Bering Sea. While realized spawning habitat is a confluence of ideal conditions (temperature, prey availability, predator refugia, etc.) for multiple life stages, the tight relationship between temperature and hatch success for gadids, namely Pacific cod, offers the opportunity to use thermally-suitable habitat (hereafter, “thermal spawning habitat”) to understand how realized spawning habitat may change across space and time (e.g., Dahlke *et al.*, 2018; Morley *et al.*, 2018; Laurel and Rogers, 2020; Cote *et al.*, 2021). We ask whether (i) the extent or area of thermal spawning habitat varies across space and time, (ii) the mean latitude of thermal spawning habitat shifts northward over time, (iii) hotspots of thermal spawning habitat are consistent across space and time, and finally, (iv) the availability of thermal spawning habitat is correlated with recruitment. To answer these questions, we use bottom temperature from a regional ocean climate model combined with an experimentally-derived relationship between hatch success and temperature. These data and temperature time series allow us to predict thermal spawning habitat suitability and associated metrics spanning 1970–2099 under two emission scenarios of the Shared Socioeconomic Pathway (SSP126 and SSP585; O'Neill *et al.*, 2016). These metrics that quantify the availability of thermal spawning habitat allow us to infer important ecological, evolutionary, and economic implications of shifts in habitat use. We additionally validate our predictions of spawning habitat based on temperature with distributional data on spawning adults and newly-hatched larvae. Ultimately, understanding how spawning habitat dynamics are shifting over time and space will help identify future issues and concerns regarding Pacific cod in the eastern Bering Sea.

Methods

The Bering Sea encompasses a latitudinal range of >1000 km between the Alaska Peninsula and the Bering Strait, transitioning from a subarctic to an arctic ecosystem from south

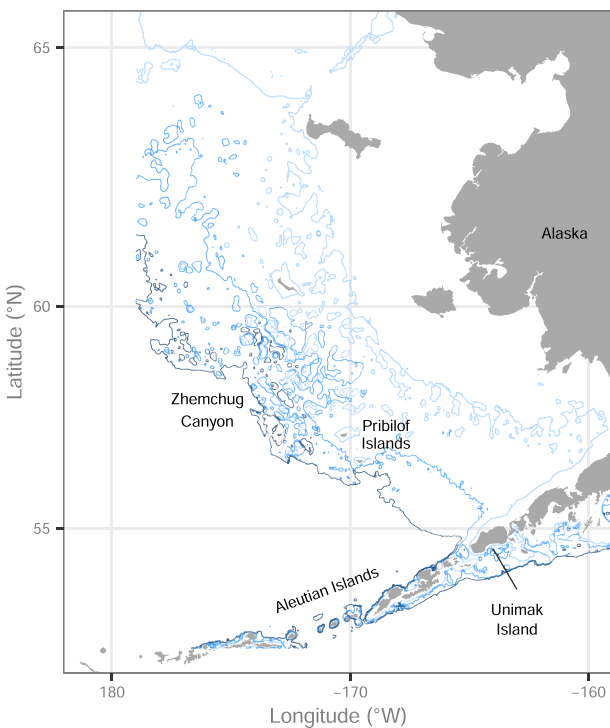


Figure 1. A map of the eastern Bering Sea, identifying locations where historical and contemporary spawning aggregations of Pacific cod have been documented (Aleutian Islands, particularly Unimak Island, along the outer shelf edge near Zhemchug Canyon, and around the Pribilof Islands, based on Neidetcker *et al.*, 2014 and Rand *et al.*, 2014). The 50, 100, and 180 m isobaths are indicated by the light blue, medium blue, and dark blue colors, respectively, and outline the inner, middle, and outer shelves. The northern and southeastern Bering Sea are delineated by the 60°N latitude (Stabeno *et al.*, 2012).

to north (Figure 1). The eastern portion is characterized by a broad, shallow (<200 m depth) shelf that stretches >500 km from shore; it can be divided into the southeastern and north-eastern Bering Sea (northern Bering Sea) at around 60°N based on differences in physical, chemical, and biological oceanography (Coachman, 1986; Stabeno *et al.*, 2012). In particular, the northern Bering Sea has a greater areal extent of sea ice and is generally characterized by colder temperatures. The southern Bering Sea can be further subdivided along isobaths into the inner (coastline to 50 m), middle (50–100 m), and outer shelves (100–180 m) based on the unique oceanographic and bathymetric characteristics of each domain (Figure 1; Coachman, 1986). The cold pool is a predominant feature of the middle shelf, although it can occasionally extend onto the inner shelf in years with extensive sea ice (Stabeno *et al.*, 2012). The outer shelf is known for its high productivity resulting from regional tidal mixing, eddies, and transverse circulation (Mizobata *et al.*, 2006).

Bottom temperature hindcasts and projections

To evaluate changes in the availability of thermal spawning habitat, we use a regional ocean model known as the Bering10K. The Bering10K model is an implementation of the Regional Ocean Modeling System (ROMS), with a domain spanning the Bering Sea and northern Gulf of Alaska and including explicit ocean, sea ice, and biogeochemical com-

ponents (Kearney *et al.*, 2020; Cheng *et al.*, 2021; Hermann *et al.*, 2021). For this study, we used several different simulations from this model. The first, which we refer to as the hindcast, covers the period of 1970–2020 and is driven by surface and boundary conditions from the Climate Forecast System operational analysis (Saha *et al.*, 2010). This is a reanalysis product, so this simulation captures the true interannual and decadal variability of the time period. The remaining simulations downscale long-term forecast simulations from the Coupled Model Intercomparison Project Phase 6 (CMIP6; Cheng *et al.*, 2021; Hermann *et al.*, 2021). The downscaled suite includes simulations forced by three different parent models: Community Earth System Model version 2-Community Atmospheric Model version 6 (CEMS2-CAM6, hereafter “CESM”), Geophysical Fluid Dynamics Laboratory Earth System Model version 4.1 (GFDL-ESM4; hereafter, “GFDL”), and MIROC-Earth System Version 2 for Long-term Simulations (MIROC-ES2L; hereafter, “MIROC”). For each parent model, we downscaled the latter portion of the historical simulation (1985–2015) and two different emission scenarios (2015–2099): SSP126 (low emission scenario) and SSP585 (high emission scenario; Cheng *et al.*, 2021; Hermann *et al.*, 2021). These particular parent models and emission scenarios were chosen to capture as much of the envelope of uncertainty from the larger CMIP6 suite as possible, given the computing and time constraints of the regional downscaling process.

From each of these simulations, we extracted weekly-averaged bottom temperature, defined as the mean temperature over the bottom (deepest) 5 m of the water column at each horizontal (latitude–longitude) location. We removed all temperature values outside of the season (January–April) and bathymetric range (shallowest than 250 m) of known spawning (Neidetcker *et al.*, 2014; Rand *et al.*, 2014). We also only included grid cells for which the Bering10K bottom temperature output has been validated against observations collected during the Alaska Fisheries Science Center’s groundfish survey, although this resulted in the removal of very few grid cells as this region is largely shallower than 250 m (Kearney *et al.*, 2020; Figure 2a–c).

Global climate models—and, thus, regionally downscaled models driven by global models—can show systematic mismatches between their output and real-world values stemming from a variety of different factors, including coarse resolution, simplified processes, and imperfect understanding of physical and ecosystem processes (Hawkins *et al.*, 2013). A small bias in simulated bottom temperature could strongly impact our projections of present-day and future thermal spawning habitat due to the narrow, fixed thermal range that defines this habitat. To mitigate these systematic differences, we adjusted the projected temperature values following Holsman *et al.* (2020). Essentially, this method calculates the bias by comparing the Bering10K results driven by the “free-running” CMIP6 global projections over the reference period with the corresponding results driven by the observed global conditions over that same period (the hindcast). The specific equation for adjusting temperature values is

$$T'_{fut, y} = T_{bind, \overrightarrow{ref}} + \frac{\sigma_{bind, \overrightarrow{ref}}}{\sigma_{fut, \overrightarrow{ref}}} (T_{fut, y} - \bar{T}_{fut, \overrightarrow{ref}}),$$

where $T'_{fut, y}$ is the adjusted projected timeseries, $T_{fut, y}$ is the raw projected time series, $T_{bind, \overrightarrow{ref}}$ is the mean of the hind-

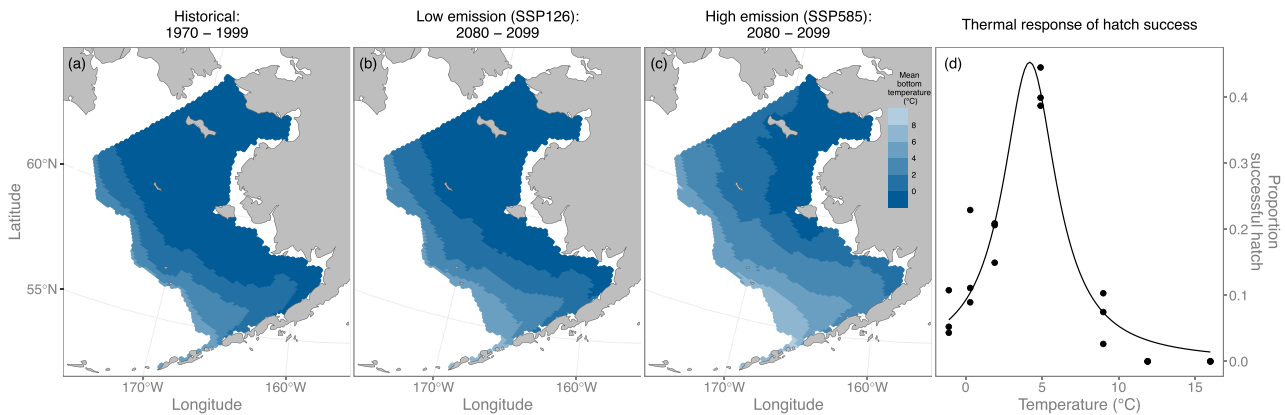


Figure 2. The predicted average bottom temperature in the eastern Bering Sea during March by the end of the century for both emission scenarios is higher than the historical period and is generally below the optimum temperature for successful hatching of Pacific cod eggs aside from the outer shelf south of $\sim 57^{\circ}\text{N}$. The bottom temperature averaged over a 20-year period in March in the past (a; historical period, 1970–1999) and at the end of the century (2080–2099) for two emission scenarios (b; low; c; high) from the Bering10K ROMS model. (d) The thermal response of hatch success measured experimentally for Pacific cod as modified from Laurel and Rogers (2020).

cast during the reference years $\overrightarrow{\text{ref}}$ (1980–2014), $\bar{T}_{\text{fut, ref}}$ is the mean of the raw projected timeseries during the reference years $\overrightarrow{\text{ref}}$, $\sigma_{\text{hind, ref}}$ is the standard deviation of the hindcast during the reference years $\overrightarrow{\text{ref}}$, and $\sigma_{\text{fut, ref}}$ is the standard deviation of the raw projected time series during the reference years $\overrightarrow{\text{ref}}$. The means and standard deviations of temperature for the reference years were averaged for a given marine sub-region as defined by the Bering Sea Ecosystem Study and Bering Sea Integrated Ecosystem Research Program (see Sigler *et al.*, 2010 for more details). We also explored how the choice of reference period affected adjusted temperature values. Specifically, we used two alternative reference periods (1990–2014 and 2006–2014) but found that the adjusted temperatures were robust to the choice of reference period (Figure S1).

Thermal spawning habitat availability

To identify temporal patterns in the availability of thermal spawning habitat and provide a basis for calculating area and mean latitude, we calculated an annual index of thermal spawning habitat suitability. We did so by combining the experimentally-derived relationship between hatch success and temperature from Laurel and Rogers (2020), as described by the Cauchy model (Figure 2d), with the hindcasts and projections of bottom temperature from the Bering10K output. This resulted in a proportion successful hatch for each grid cell for each week from January to April for each year spanning 1970–2099; these values were averaged on a monthly and then yearly basis and were standardized on a scale from zero to one (following Dahlke *et al.*, 2018; Cote *et al.*, 2021).

To understand how the area thermally suitable for spawning changes, we calculated the extent or area of thermal spawning habitat. For this, following Dahlke *et al.* (2018) and Cote *et al.* (2021), we summed the area of all grid cells that reached two threshold values—0.9, “core thermal spawning habitat area” and 0.5, “potential thermal spawning habitat area”—at any point across the time period examined (i.e., if a single month reached the threshold or two to four months cumulatively reached the threshold). We chose these thresholds

based on those in other studies that examine thermal spawning habitat availability (e.g., Dahlke *et al.*, 2018; Cote *et al.*, 2021). This yielded yearly area estimates for January to April for both core and potential thermal spawning habitat area. Third, we calculated the mean latitude of both core and potential thermal spawning habitat area for each year (i.e., for core area, mean latitude would equal the average latitude of all grid cells for which standardized hatch success was >0.9) to understand whether core and potential thermal spawning habitat area are shifting northward, as is commonly seen across marine species as temperatures rise (Pinsky *et al.*, 2013). Finally, we examined the consistency of locations harbouring core and potential thermal spawning habitat area over space and time, which helps us understand how reliable or predictable a particular location is for successful spawning. To do so, we calculated the percentage of years a given grid cell was greater than or equal to the two threshold values (0.9 and 0.5, or core and potential thermal spawning habitat area).

Correlating thermal spawning habitat with recruitment

To determine whether the availability of thermal spawning habitat relates to year-class strength (a proxy for recruitment), we obtained estimates of abundance of age-0 Pacific cod and associated error from the stock assessment model, an age-structured model fit to survey and fishery data (Thompson *et al.*, 2021). We then estimated the Pearson’s correlation coefficient for the relationship between age-0 abundance (log-transformed) and the annual index of thermal spawning habitat suitability (averaged across space for each year) and area (both core and potential). We also calculated the ratio between the number of (age-0) recruits and spawning stock biomass and assessed whether this ratio was correlated with the annual index of thermal spawning habitat suitability and area of core and potential thermal spawning habitat.

Validating spawning location

To validate our predictions of spawning habitat based on temperature, we examined the distribution of newly-hatched larvae around the months of known spawning (January–April)

in the eastern Bering Sea (Neidetcher *et al.*, 2014; Rand *et al.*, 2014). Specifically, we mapped the distribution of larval density from ichthyoplankton surveys conducted by NOAA Alaska Fisheries Science Center's Ecosystems and Fisheries-Oceanography Coordinated Investigations (EcoFOCI) for all years ($n = 24$; 1979, 1991, 1993–1997, 1999, 2000, 2002, 2003, 2005–2017) and stations available. These surveys use paired bongo nets with 333 or 505 m mesh and sample via oblique tows from the surface to 100 m depth (or from 10 m off the bottom for shallower water; Matarese *et al.*, 2003). We limited these data to the months of April–June as larvae were most frequently caught during these months and included only individuals <6 mm in length (larvae are ~ 4 mm in length upon hatching and grow ~ 0.30 – 0.40 mm per day; Laurel *et al.*, 2008). Additionally, we compare our predictions of spawning habitat based on temperature to the distributions of spawning fish reported by Neidetcher *et al.* (2014) and recent tagging work on adult Pacific cod in the Bering Sea during the winter (Thompson *et al.*, 2021).

Sensitivity analyses

Although the shape of the hatch success–temperature relationship from Laurel and Rogers (2020) is consistent with studies on other marine fishes (i.e., survival rates are highest across a narrow range of temperatures and the shape is similar to a Gaussian or Cauchy distribution; Tsoukali *et al.*, 2016), and those specifically on Pacific cod from other geographic regions (Japan: Bian *et al.*, 2014, 2016; Strait of Georgia: Alderdice and Forrester, 1971), we examine how uncertainty in this relationship affects our predictions of the availability of thermal spawning habitat. To do so, we bootstrapped the three parameters from the Cauchy model 500 times, selected ten random subsets of parameter combinations, and then estimated the thermal spawning habitat suitability index for each of these combinations. We then fit linear regressions for the hindcast period and both emission scenarios of the projection period to compare with the linear trend of the thermal spawning habitat suitability time series calculated from parameters reported by Laurel and Rogers (2020). Because Laurel and Rogers (2020) also examined the fit of the hatch success–temperature data to a Gaussian distribution, we repeated these sensitivity analyses using a Gaussian distribution (bootstrapped parameters from a Gaussian model, calculated thermal spawning habitat suitability indices, and fit linear regressions to examine the trend in thermal spawning habitat suitability over time). The absolute scale of thermal habitat suitability varied slightly depending on the value of the parameters (Figures S2, S3). However, the linear trend of thermal habitat suitability over time as estimated from the Cauchy models did not vary, and while the Gaussian models tended to estimate faster rates of increase (slopes of the linear trend), the slopes overlapped with those from the Cauchy models (Figures S4, S5). Thus, we present the results using the hatch success–temperature relationship from Laurel and Rogers (2020).

Results

Bottom temperature hindcasts and projections

Winter bottom waters on the southeastern Bering Sea shelf are predicted to warm considerably by the end of the cen-

tury (Figure 2a–c, Figure 3a and b, Figure S6, S7). Prior to the beginning of the 21st century, environmental conditions in the southeastern Bering Sea, including bottom temperature, showed high interannual variability. From the early 2000s to the present, the environmental and oceanographic conditions for consecutive years were relatively similar, leading to the categorization of years into “warm” or “cold” stanzas lasting four to six years (*sensu* Stabeno, *et al.*, 2012). In the future, this pattern of alternating warm and cold stanzas persists until around the middle of the century, after which temperature increases steadily and no more “cold” years/stanzas are predicted to occur (Figure 3a and b). In contrast to the southeastern Bering Sea, the northern Bering Sea has historically been less thermally variable as it is dominated by a high areal ice extent for almost half of the year, which causes bottom temperatures to remain cold, a trend that persists even into the future (Figure 2b and c, Figure S6, S7). Indeed, the winter bottom temperatures for the entire northern Bering Sea remain below 0°C through the end of the century under the low emission scenario, and under the high emission scenario, much of the region remains below 0°C with the western edge warming to around 2°C (Figure 2b and c, Figure S7).

Over the 50-year historical period, yearly- and spatially-averaged bottom temperature varied up to 1.9°C across the eastern Bering Sea shelf but did not increase over time (mean slope and 95% confidence intervals [CI] = 0.006, -0.003 – 0.014 ; Figure 3a and b). In contrast, the projected bottom temperature under both emission scenarios did increase over time (mean slope and 95% CI for low = 0.009, 0.006– 0.012 and high = 0.37, 0.29– 0.044 emission scenarios; Figure 3a and b). By mid-century, bottom temperature is predicted to increase up to 2.9°C and 3.8°C under the low and high emission scenario, respectively, and by the end of the century, up to 3.5°C and 5.0°C under the low and high emission scenario, respectively. Under both emission scenarios, the CESM model predicts the greatest temperature increases while the other two models show more modest increases (Figure 3a and b). Such model discrepancy has been documented; for example, Cheng *et al.* (2021) show that the CESM model predicts temperatures that are warmer than observations while the GFDL and MIROC models predict temperatures that are colder than observations. These differences in temperature projections are due, in part, to differences in the extent of seasonal sea ice among models (Cheng *et al.*, 2021).

Spatially, the (yearly-averaged) bottom temperature on the outer shelf edge, particularly the southern shelf edge, remained warmer ($\sim 4^{\circ}\text{C}$) than the middle or inner shelf during the historical period. Over this time, warmer bottom temperatures expanded from the outer shelf edge to the middle and even inner shelf, primarily in the southeastern areas of both domains (Figure S6). The middle and inner shelves north of 57°N generally remained cooler ($<0^{\circ}\text{C}$; Figure S6). In the future, warmer bottom temperatures are projected to spread across the shelf from the outer edge to the inner shelf, primarily in the southeast, particularly south of 59°N (Figure S7). Similar to the historical period, the middle and inner shelves north of 57°N – 60°N remain cooler, even by the end of the century (Figure S7).

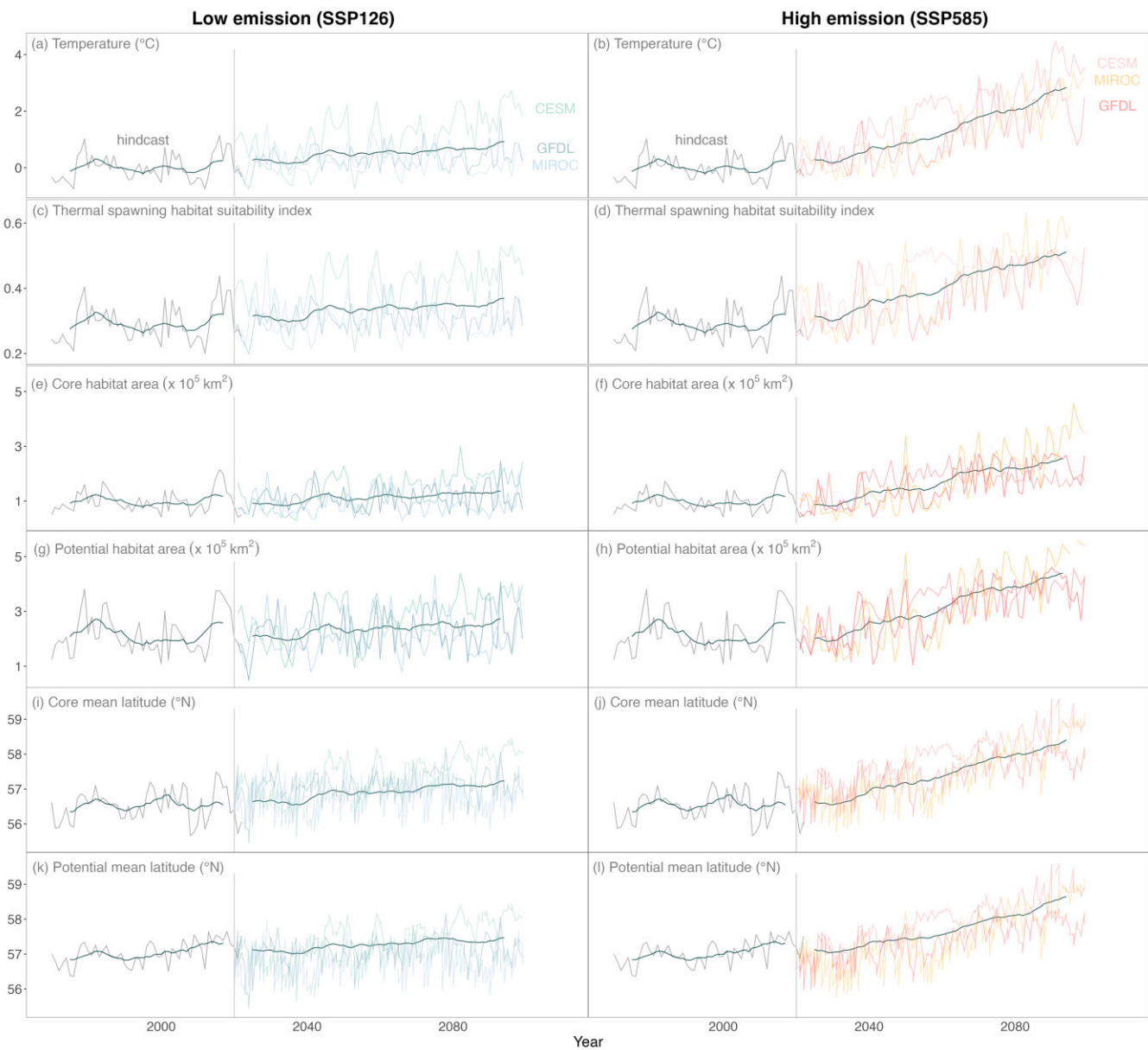


Figure 3. Temperature, thermal spawning habitat suitability index, area, and mean latitude are highly variable but increase over time by the end of the century, particularly if no climate mitigation occurs. Time series of (a and b) bottom temperature, (c and d) index of Pacific cod thermal spawning habitat suitability, (e–h) thermal spawning habitat area, and (i–l) mean latitude averaged over January to April of each year for all three global climate models regionally downscaled for the Bering10K ROMS model (colors, see text in panels (a) and (b) for both low (left panels; a, c, e, g, i, and k) and high (right panels; b, d, f, h, j, and l) emission scenarios. In all panels, the vertical gray line indicates 2020, and the smoothed gray line in the foreground is the 11-year running mean of the hindcast and projection of each respective variable.

Thermal spawning habitat suitability and associated metrics

Index of thermal spawning habitat suitability

The dynamics of bottom temperature over space and time translate into similar dynamics of thermal spawning habitat suitability for both the historical and future periods (Figure 3c and d). Overall, the thermal spawning habitat suitability index, while highly variable over the entire period, is projected to increase by the end of the century. Such increases in thermal spawning habitat suitability are due to the bottom temperatures approaching, but not exceeding, the optimum temperature for successful hatching across large regions of the eastern Bering Sea shelf.

From 1970–2020, the thermal spawning habitat suitability index varied considerably (Figure 3c and d). As with temperature during this time, the thermal spawning habitat suitability index was more similar in consecutive years until the thermal regime switched (i.e., from a cold to warm stanza). However, there was no significant directional trend in thermal spawning habitat suitability over the course of the entire historical period, likely due to the colder bottom temperatures remaining on the eastern Bering Sea shelf (mean slope and 95% CI = 0.0007, -0.0003–0.002). In the future, the thermal spawning habitat suitability index is predicted to rise, particularly under the high emission scenario (mean slope and 95% CI for the low = 0.0008, 0.0004–0.001 and high = 0.003, 0.002–0.004 emission scenario; Figure 3c and d). Indeed,

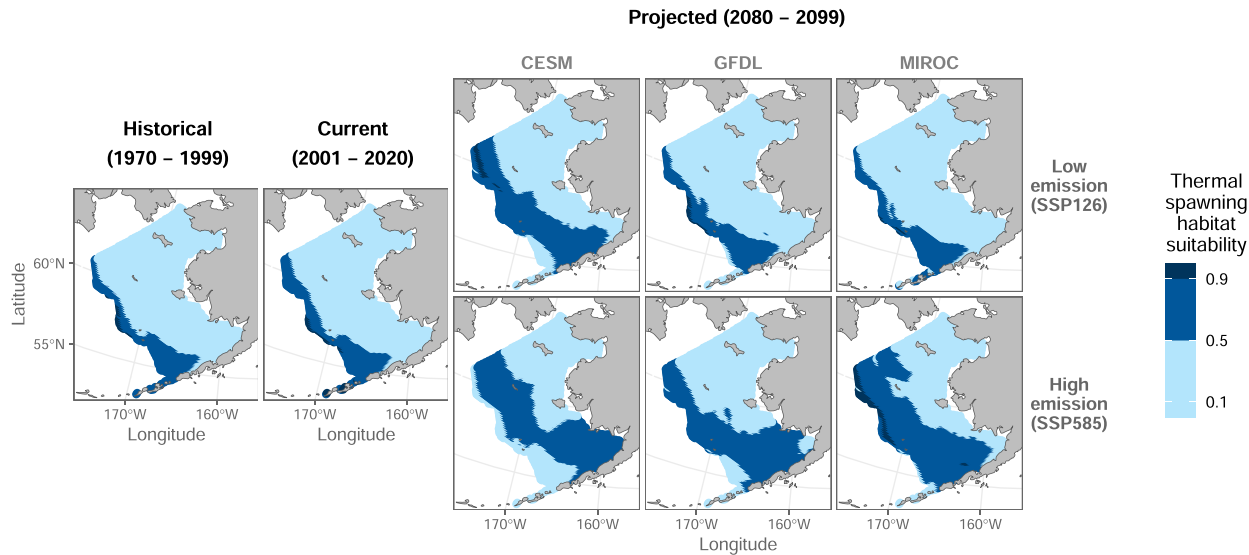


Figure 4. Core and potential thermal spawning habitat are concentrated on the outer shelf and shift and expand spatially towards the middle shelf by the end of the century, particularly under the high emission scenario. Maps of both core (thermal spawning habitat suitability ≥ 0.9) and potential (≥ 0.5) thermal spawning habitat for the historical (1970–1999), current (2001–2020), and last 20 years of the projected period (2080–2099; indicated by the black bold text labels above the plots) for Pacific cod. Thermal spawning habitat suitability was averaged across each respective time period and for the last 20 years of the projected period; maps are shown for each global climate model (columns, see text) and emission scenario (rows, see text).

compared to 1970, the thermal spawning habitat suitability index is predicted to increase by over 119% and 179% under the low and high emission scenarios, respectively. As with the projected temperature time series, the CESM model predicts greater increases in the thermal spawning habitat suitability index compared to the GFDL and MIROC models (Figure 3c and d).

Area of thermal spawning habitat

Overall, the area of core (≥ 0.9) and potential (≥ 0.5) thermal spawning habitat did not increase over the historical period (mean slope and 95% CI for core = 0.002, $-0.003-0.006$ and potential = 0.002, $-0.003-0.007$ thermal spawning habitat area). However, the area of both core and potential thermal spawning habitat is projected to increase in the future under the low (mean slope and 95% CI for core = 0.003, $0.001-0.004$ and potential = 0.003, $0.002-0.005$) and high (mean slope and 95% CI for core = 0.008, $0.005-0.01$ and potential = 0.009, $0.006-0.01$) emission scenarios (Figure 3e–h).

Spatially, the majority of core thermal spawning habitat area during the historical period was concentrated on the outer shelf edge. In contrast, potential thermal spawning habitat area increased and expanded across the shelf during this time, from the outer shelf onto the middle and inner shelves south of $\sim 57^{\circ}\text{N}$ (Figure 4). During the historical period, the entire northern Bering Sea remained below the threshold of potential thermal spawning habitat (≥ 0.5) due to the temperature remaining below 0°C (Figure 4). In the future, thermal spawning habitat area—particularly potential—is projected to increase and expand across the eastern Bering Sea onto the middle and inner shelves by the end of the century, especially under the high emission scenario (Figure 4). For two of the global climate models—CESM and GFDL, both potential and core thermal spawning habitat areas shift slightly in-

shore, occupying the southern extent of the middle and even inner shelves (south of $57^{\circ}\text{N}-60^{\circ}\text{N}$, Figure 4). Similar to the historical time period, the northern Bering Sea is not projected to become thermally suitable for spawning by the end of the century under any model or emission scenario, as it remains below the range of temperatures that confer a high probability of hatch success (Figure 4).

Mean latitude of thermal spawning habitat suitability

The mean latitude of both core and potential thermal spawning habitat area shifts northward over time, particularly under the high emission scenario (Figure 3i–l, Figure 5). Compared to the mean latitude for core and potential thermal spawning habitat area averaged across the hindcast period (1970–2020), the projected increase in mean latitude by the end of the century across the three parent models is around two degrees latitude under the high emission scenario. Under both emission scenarios, projected increases in mean latitude are slightly greater for core thermal spawning habitat compared to potential (Figure 3i–l). Finally, the average location of both core and potential thermal spawning habitat—as measured by the mean latitude and longitude—shifts north over time, and the spread of locations narrows from east to west (Figure 5).

Consistency of thermal spawning habitat suitability

Thermal spawning habitat suitability values are relatively consistent in a given location across shorter time periods (decades), but areas that are consistently thermally suitable shift slightly and expand across the shelf over the course of the entire time frame (130 years), similar to the changes in thermal spawning habitat area (Figure 6). During the historical period, the outer shelf edge was consistently core thermal spawning habitat, as $\sim 75\%$ or more of years had a thermal spawning habitat suitability index ≥ 0.9 . For locations

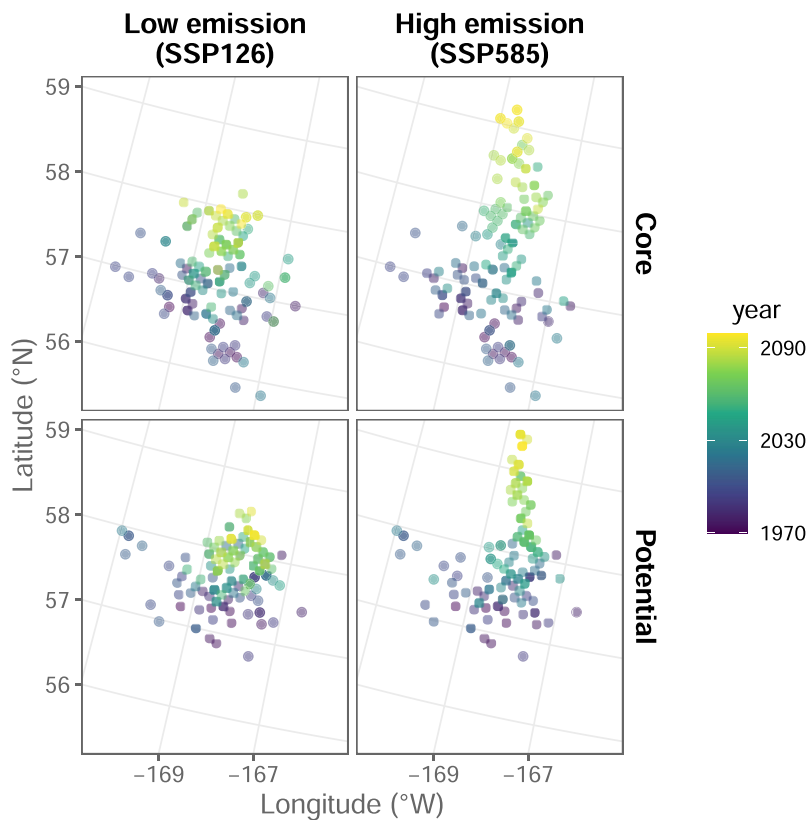


Figure 5. The mean latitude ($^{\circ}$ N) and longitude ($^{\circ}$ W) of both core and potential thermal spawning habitat is shifting northward over time and narrowing from east to west. The yearly-averaged mean latitude and longitude of both core (thermal spawning habitat suitability ≥ 0.9 , top row) and potential (≥ 0.5 , bottom row) thermal spawning habitat for Pacific cod under low (left column) and high (right column) emission scenarios. For each emission scenario, the projected mean latitude and longitude change is averaged across the three global climate models.

just east of the shelf break, ~ 25 –75% of years reached the threshold for core habitat (Figure 6). In the future, areas that are consistently thermally suitable core habitat shift slightly inshore onto the middle shelf over time, particularly south of 57° N. Across this time frame (2021–2099), grid cells that were core habitat the entire time ($\sim 100\%$ of years) are typically found on the northern end of the outer shelf edge. The percentage of years a given grid cell reached the core habitat threshold declined towards the southern portion of the outer shelf edge (although the high emission scenario of the MIROC model predicts high consistency on the middle shelf). While both emission scenarios predict similar patterns of consistency for core thermal spawning habitat area, the high emission scenario predicts a further shift inshore (Figure 6). For potential habitat (thermal spawning habitat suitability index ≥ 0.5), areas that are consistently thermally suitable during the historical period remained so across all years spanning 1970–2020. These regions of historic thermal suitability expanded inshore from the outer shelf edge and from the southern portion of the middle shelf onto the southern portion of the inner shelf (Figure 6). This pattern continues in the future, as potential habitat is consistently found on the middle shelf for many years, and under the high emission scenario, the southern region of the inner shelf (Figure 6). Similar to the pattern for core habitat, the outer shelf edge becomes less consistently thermally suitable in terms of potential habitat over time (i.e., fewer years reach 0.5), particularly under both scenarios of

the CESM model, as areas that are consistent shift inshore (Figure 6).

Thermal spawning habitat suitability and recruitment

Over the time span of years in which abundance estimates of age-0 fish were available (1977–2020), we did not find a significant relationship between age-0 abundance and the spatially-averaged index of thermal spawning habitat suitability (Pearson's correlation coefficient = -0.16 , $p = 0.29$; Figure 7) or for core (Pearson's correlation coefficient = -0.20 , $p = 0.21$) or potential area (Pearson's correlation coefficient = -0.19 , $p = 0.24$). We also did not find a relationship when we examined the correlation between the ratio of recruit abundance to spawning stock biomass and the index of thermal spawning habitat suitability or area (Pearson's correlation coefficient = -0.08 , -0.19 , and -0.17 , respectively, and $p = 0.59$, 0.23 , and 0.28 , respectively).

Validating spawn location

The distributions of both newly-hatched larvae and spawning adults validated our predictions of spawning habitat based on temperature. Specifically, catches of small-sized larvae were concentrated along the outer shelf and along the Aleutian Islands (Figure 8), overlapping with the locations predicted to be sites of spawning based on temperature (Figure 4, “historical” and “current” panels). The distribution of fish in pre-spawning, spawning, and spent stages is typically concen-

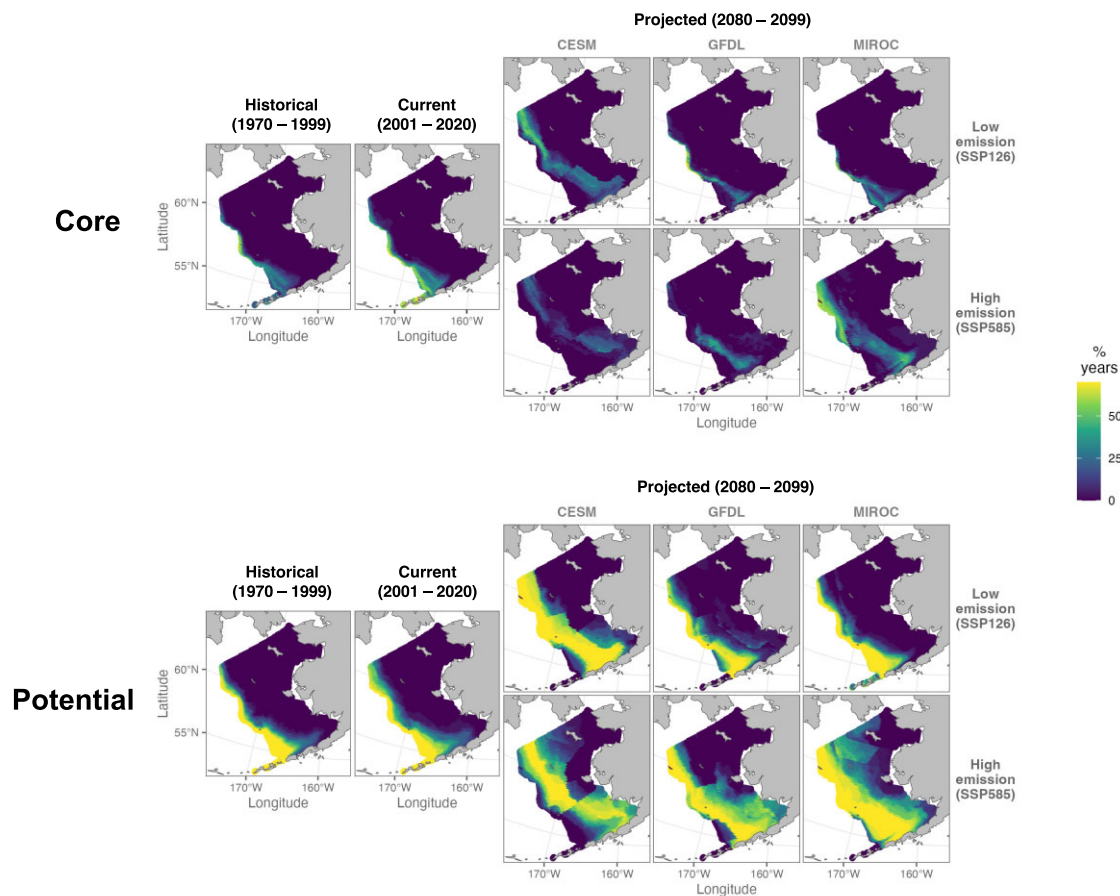


Figure 6. Core and potential thermal spawning habitat are relatively consistent across shorter time periods (decadal scale) but do expand and shift spatially by the end of the century. Maps of the consistency of Pacific cod core (thermal spawning habitat suitability ≥ 0.9 , top panel) and potential (≥ 0.5 , bottom panel) thermal spawning habitat for the historical period (1970–1999) and current period (2001–2020) compared to that projected by the end of the century (2080–2099) for all three global climate models (columns of the projected maps) under both low and high emission scenarios (rows of the projected maps).

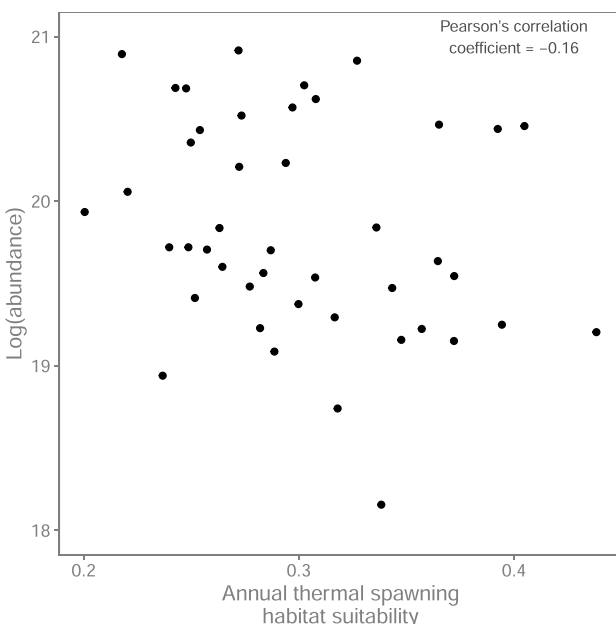


Figure 7. No relationship exists between the annual index of thermal spawning habitat suitability for Pacific cod and the modeled (log) abundance of age-0 fish from 1977–2020.

trated on the outer shelf edge and along the Aleutian Islands, particularly around Unimak Island; additionally, recovery locations of tagged adult Pacific cod during the height of the spawning season (February and March) were concentrated along the outer shelf edge and less so, near Unimak Island (Neidetcher *et al.*, 2014; Thompson *et al.*, 2021).

Discussion

Overall, our work suggests that changing thermal conditions in the eastern Bering Sea have affected and will continue to affect the spawning habitat dynamics of Pacific cod. While the availability of thermally-suitable spawning habitat—in terms of a yearly index of thermal spawning habitat suitability and areal extent—is predicted to increase by the end of the century, our projections suggest that historical spawning sites will become less thermally suitable over time and thermal spawning habitat will shift slightly northward. Despite the tight mechanistic relationship between temperature and hatch success, which allows us to use bottom temperature to successfully predict the location of historical and contemporary spawning sites, our work suggests that the availability of thermal spawning habitat as predicted here likely has not constrained regional stock productivity (recruitment) in the past, nor is it likely to in the future. However, the spatial shift in ther-

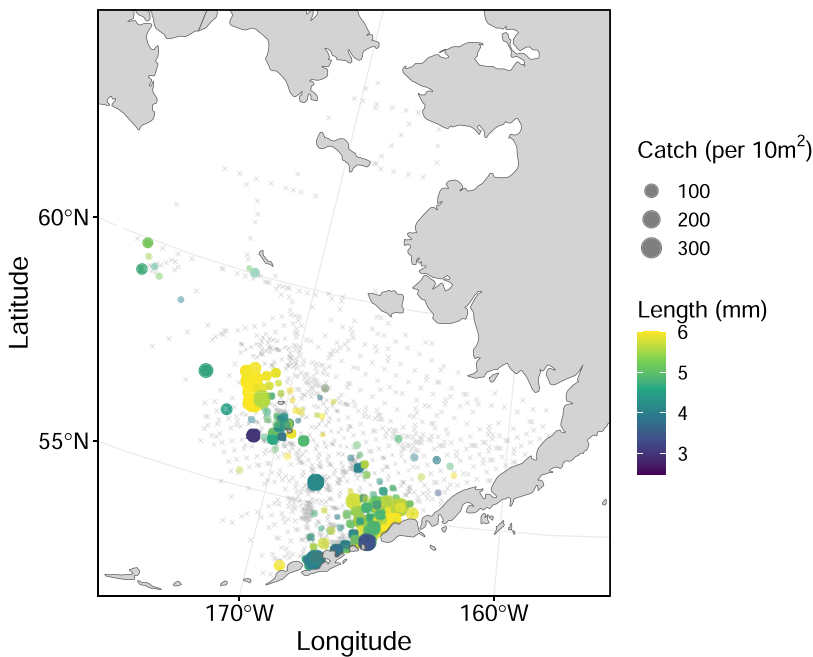


Figure 8. Observations of larval catches validate our predictions of thermal spawning habitat based on temperature. Empirical observations of the distribution of small Pacific cod larvae (< 6 mm) from fisheries surveys conducted in the Bering Sea during April–June for as many years as possible (1979, 1991, 1993–1997, 1999, 2000, 2002, 2003, and 2005–2017). Also shown (indicated by the grey x's) are the station locations for which small larvae were not caught.

mal spawning habitat by the end of the century may have other (and possibly unanticipated) consequences. For example, these consequences may include a change in the migration distance from summer feeding areas to spawning sites and novel species interactions, as well as socioeconomic impacts such as changes in cost and effort for the fishery (Sumaila *et al.*, 2011; Watson and Haynie, 2018; Rogers *et al.*, 2019). Although distributional shifts are one of the most well-known responses to warming (Pinsky *et al.*, 2013; Burrows *et al.*, 2014; Pinsky *et al.*, 2020), our work highlights how such shifts may be size- and season-dependent and couples a mechanistic relationship with global climate model output to understand how thermal spawning habitat has varied in the past and forecast how it may vary in the future.

We found an overall increase in the availability of thermal spawning habitat, as indicated by both the increase in the thermal spawning habitat suitability index and spatial extent of both core and potential thermal spawning habitat. Expansions of habitat area with warming, just as contractions, have been documented for many species (Bennie *et al.*, 2013; Kleisner *et al.*, 2017). Such changes in thermal habitat can depend on life stage; for example, by the end of the current century, thermally-suitable habitat for spawning adults of Nassau grouper is projected to decline by 82% compared to 46% for non-spawning adults (Asch and Erisman, 2018). Changes in thermal habitat for earlier life stages and their effects are less well documented. For gadids specifically, both increases and decreases in thermal spawning habitat with warming (based on experimentally-derived relationships between temperature and egg survival as used here) have been found, with differences attributed to the nature of the temperature changes and life histories of the individual species (i.e., subarctic vs. arctic species, shape of the thermal response curve, nature of temperature changes in the region; Dahlke *et al.*, 2018; Laurel

and Rogers, 2020; Cote *et al.*, 2021). For Polar cod, an arctic species with egg survival highest in waters < 3°C, thermal spawning habitat is projected to decrease in both the Norwegian Sea (by ~67% in the warmest areas) and the Labrador Sea and Northwest Atlantic (by ~21%) by the end of the century (Dahlke *et al.*, 2018; Cote *et al.*, 2021). Atlantic cod, a subarctic species whose eggs have a broader range of temperatures suitable for survival compared to both Polar and Pacific cod (highest survival between 0°C and 9°C), can expect regional increases and decreases in thermal spawning habitat by the end of the century (Dahlke *et al.*, 2018; Cote *et al.*, 2021). Using the same experimentally-derived relationship between temperature and egg survival as used here, Pacific cod (or Greenland cod, *Gadus ogac*, as named in the Atlantic despite no genetic differentiation; Coulson *et al.*, 2006) thermal spawning habitat suitability is expected to increase in the Labrador Sea by the end of the century (by 19%; Cote *et al.*, 2021). However, decreases in thermal spawning habitat have also been documented for this species following a marine heatwave (Laurel and Rogers, 2020). We found large increases in the availability of thermal spawning habitat for Pacific cod in the eastern Bering Sea at mid-century with warming temperatures under both emission scenarios. Over time, the increases in temperature on the middle and inner shelves facilitate the expansion of thermal spawning habitat onto the shelf and translate into increases in area that may be enough to counter the decreases on the outer shelf edge.

The implications of this increase in the availability of thermal spawning habitat are less well understood. Although predicting distributions and habitat use from temperature has shown to be quite successful across regions, species, and time frames, ecological characteristics such as distributions are complex and are often the result of many interactive factors (Pörtner and Farrell, 2008; Pinsky *et al.*, 2013; Sunday *et*

al., 2019). Indeed, temperature is one of many factors that affect the suitability of habitat as realized spawning habitat is thought to represent a confluence of ideal conditions (e.g., prey availability, refugia from predators, connectivity between spawning sites and nursery grounds) for multiple life stages (spawning adults, larvae, eggs) in addition to temperature (Ciannelli *et al.*, 2015, 2021). While we note that our predictions of spawning habitat based on temperature alone do match observations of known historical and contemporary spawning sites based on the distribution of adults and newly-hatched larvae, other variables could be included to refine predictions of where fish may spawn in the future (Neidetcher *et al.*, 2014; Laurel *et al.*, 2021; Thompson *et al.*, 2021). For example, including data on substrate and sediment types would be ideal for Pacific cod, as they are demersal spawners. In the case of the Bering Sea, however, coarse sediment data suggests that much of the outer and middle shelves are characterized by similarly-sized (large grain size) sediments, suggesting that if Pacific cod spawning habitat dynamics are closely tied to substrate type, shifts inshore would offer similar substrates and are unlikely to be a constraint (Laman *et al.*, 2022). Oxygen would be another important variable to consider, but currently, we lack information on how hatch success relates to oxygen availability. Additionally, our sensitivity analyses revealed that while the trend in thermal habitat suitability is quite robust, the absolute amount of such habitat may be slightly higher or lower.

Despite our finding of an overall increase in the availability of thermal spawning habitat that shifts slightly northward, we also found that sites historically suitable for spawning based on temperature are not projected to be so by the end of the century. Specifically, the outer shelf edge—a hotspot for current and past spawning—is projected to become warmer than optimal for successful development and hatching of eggs by the middle of the century. Because spawning habitat reflects a combination of many conditions, a shift in spawning location may impact the survival and transport of newly-hatched larvae (Agostini and Bakun, 2002; Ciannelli *et al.*, 2015). If spawning locations shift spatially (or temporally) based on the physiological limits of eggs, new habitats (or the same habitat at a different time) may not offer the necessary conditions and other requirements and characteristics of spawning habitat. One possible advantage to the predictions of increased thermal spawning habitat on the middle and inner shelves is the potential for overlap with habitat identified as important for juvenile survival (Farley *et al.*, 2016; Laurel *et al.*, 2021). Of course, this assumes that juvenile habitat quality will remain high in these middle and inner shelf regions, which will need to be evaluated with further work. Likewise, larval dispersal from spatially-shifting spawning grounds would be important to consider. Finally, shifts in spawning aggregations have the potential to affect the logistics and operational costs of fisheries that target such aggregations (Pinsky and Fogarty, 2012; Asch and Erisman, 2018; Dahlke *et al.*, 2018). In the Bering Sea, for example, a major fishery for Pacific cod occurs in the winter and is centred on the outer shelf edge and along the Aleutians, sites known to be historically important for spawning adults (Neidetcher *et al.*, 2014; Rand *et al.*, 2014).

While a relatively large area was consistently thermally suitable (in terms of percentage of years) for spawning over short time frames, the locations of consistent habitat shifted over longer periods. Specifically, the middle and inner regions of

the shelf became more thermally suitable over time, and the outer shelf edge, particularly the southern portion, became less thermally suitable over time. Based on current, yet limited knowledge, Pacific cod spawning aggregations occur in the same locations from year to year (Neidetcher *et al.*, 2014; Rand *et al.*, 2014). Such patterns indicate that spawning habitat and early life stages of this species are spatially constrained, meaning that they are limited to specific locations that provide the conditions and characteristics for spawning and larval survival (Ciannelli *et al.*, 2015, 2021). Indeed, for a species to successfully reproduce, the conditions and characteristics of spawning habitat needed to maximize offspring survival must be met over the long term, and not fluctuate greatly from year to year (Ciannelli *et al.*, 2021). Our finding that the locations of consistent thermally-suitable habitat are similar for shorter periods but do shift over the course of the century may indicate reduced reproductive success in the future. For example, Pacific cod spawning habitat seems to be spatially constrained, but warming temperatures may cause it to shift geographically. Alternatively, reproductive success may be less affected if the timing of spawning (spawning phenology) shifts, as is found in other species (Rogers and Dougherty, 2019). However, we were unable to assess this here due to a lack of detailed data on the timing of reproduction of Pacific cod in the Bering Sea.

We found no relationship between recruitment and thermal spawning habitat suitability. This is likely because the availability of thermal spawning habitat has not limited Pacific cod's reproductive potential in the eastern Bering Sea. Other work that has assessed the link between thermal spawning habitat availability and population dynamics has found a positive relationship between the two, but only in cases where thermal habitat shrunk (as opposed to increased, as we found here; Dodson *et al.*, 2019; Laurel and Rogers, 2020). For example, Laurel and Rogers (2020) found that a reduction of thermal spawning habitat for Pacific cod following a heatwave in the Gulf of Alaska, and thus poor hatch success, was linked to lower abundance of larvae, age-0 juveniles, and age-3 recruits. Likewise, Dodson *et al.* (2019) revealed that larval abundance of herring (*Clupea harengus*) was higher when water temperatures were optimal for hatch success over a 23-year time series. While not based on the availability of thermal habitat specifically, a loss of settlement habitat due to warming for some coral reef fish—habitat supporting survival of early life stages—is thought to have contributed to declines in abundance (Munday *et al.*, 2008). The relationship between thermal spawning habitat availability and recruitment or productivity may be nonlinear; for example, Laurel *et al.* (*in review*) found a threshold response such that recruitment failure was only evident when thermal spawning habitat metrics fell below a certain value. To our knowledge, studies that have predicted increases in thermal spawning habitat, as we found here (e.g., Dahlke *et al.*, 2018; Cote *et al.*, 2021), have not assessed whether this increase was related to recruitment. In the case of Pacific cod in the eastern Bering Sea, it appears that other factors, and not the availability of thermal spawning habitat, are related to recruitment and stock dynamics (Farley *et al.*, 2016). Indeed, recruitment of Pacific cod in the Bering Sea, and other groundfish species, is related to a host of factors, including climatic variability (e.g., sea ice, winds) and diet and species interactions (predation, prey availability), to name a few (Hollowed *et al.*, 2001; Houde, 2008; Rogers *et al.*, 2021). Additionally, larval dispersal and juvenile habitat may be affected

if spawning habitat shifts spatially. Thus, while the availability of thermal spawning habitat has not affected Pacific cod recruitment, warming will undoubtedly affect Pacific cod and other species in other, possibly unanticipated, ways.

Predicting distributional shifts in response to warming—one of the “universal” responses to climate change—is a central challenge as such shifts have far-reaching biological and socioeconomic implications (Pinsky *et al.*, 2020). Many studies rely on correlational relationships between environmental and biological variables such as abundance or biomass (e.g., Morley *et al.*, 2018). Mechanistic-based approaches are gaining traction and improve upon the uncertainty in correlational predictions (Evans *et al.*, 2015; Cote *et al.*, 2021). For example, a species may not encounter the entire range of temperatures they can physiologically withstand if solely examining distributional data (Kearney *et al.*, 2020). Additionally, mechanistic-based approaches allow us to better understand why certain distributional shifts may occur (Cheung *et al.*, 2013; Deutsch *et al.*, 2020). Finally, different life stages typically have different thermal sensitivities, resulting in ontogenetic changes in distributions that are linked to habitat use (Barbeaux and Hollowed, 2018; Dahlke *et al.*, 2020). Predicting distribution based on correlative approaches alone is often limiting in terms of what life stages can be observed (Pinsky *et al.*, 2013; Morley *et al.*, 2018; Fredston *et al.*, 2021). While such approaches work for some life stages (juveniles, adults), they are difficult to extend to early life stages (eggs). Because early life stages may act as a bottleneck to a species’ ability to adapt to warming and other changing environmental conditions (Asch and Erisman, 2018; Dahlke *et al.*, 2018, 2020; Ciannelli *et al.*, 2021), understanding how warming will affect them is a critical step in understanding, predicting, and mitigating the effects of a changing climate. Here, we make use of a mechanistic relationship between hatch success and temperature and leverage regional dynamical downscaling forced by global climate model simulations that offer projections of temperature to understand how thermal spawning habitat—and possibly the distribution of spawning adults, eggs, and newly-hatched larvae—has changed in the past and will continue to do so in the future. Future work could extend our framework to include other variables that are important for successful spawning, e.g., oxygen and sediment type as stated earlier. As polar regions like the Bering Sea are rapidly changing environmentally (Zhang, 2005; Stabeno and Bell, 2019), predictions such as ours will facilitate preparing for future uncertainty.

Acknowledgements

LR acknowledges NPPR project #2003. JSB acknowledges NSF grant number 2109411. We thank the Plankton Sorting and Identification Center (Poland) and Alaska Fisheries Science Center (USA) for their taxonomic expertise, as well as the countless researchers who have collected the data used here on EcoFOCI cruises. We also thank NOAA’s Alaska Integrated Assessment Program (IEA) and the Alaska Climate Integrated Modeling project (ACLIM) for the production and public sharing of high resolution downscaled ROMSNPZ projections and hindcasts for the Bering Sea and thank the ACLIM and EcoFOCI teams for feedback and discussions on the broader application of this work. This paper is contribution EcoFOCI-1039 to NOAA’s Ecosys-

tems and Fisheries-Oceanography Coordinated Investigations Program.

Supplementary Data

Supplementary material is available at the ICESJMS online version of the manuscript.

Conflict of interest

The authors declare that they have no competing interests.

Data availability

We place no restrictions on data or code availability. The hindcast and CMIP6 projections of the Bering 10K ROMS bottom temperature output are publicly available on <https://data.pmel.noaa.gov/aclim/thredds/catalog/catalog.html>. Code for accessing the data are available through the ACLIM project’s Github repository (<https://github.com/kholzman/ACLIM2>). All code to bias-correct temperature output and subsequently calculate hatch success and all other metrics used in this study are available on GitHub at <https://github.com/jennybigman/Pcod-Bering-Sea>.

Author contributions

Conceptualization (JSB, BJL, LAR); Methodology (JSB, BJL, LAR); ROMS model development and data curation (KK, AH, WC, KH); Formal analysis (JSB); Writing—Original draft (JSB); Writing—Review & Editing (BJL, KK, AH, WC, KH, LAR); Visualization (JSB); Validation (LAR); Resources (BJL, KK, AH, WC, KH, LAR); Supervision (BJL, LAR); Funding Acquisition (BJL, LAR).

References

Agostini, V. N., and Bakun, A. 2002. Ocean triads’ in the Mediterranean Sea: physical mechanisms potentially structuring reproductive habitat suitability (with example application to European anchovy, *Engraulis encrasicolus*). *Fisheries Oceanography*, 11: 129–142.

Alderdice, D. F., and Forrester, C. R. 1971. Effects of Salinity, Temperature, and Dissolved Oxygen on Early Development of the Pacific Cod (*Gadus macrocephalus*). *Journal of the Fisheries Research Board of Canada*, 28: 883–902.

Asch, R. G., and Erisman, B. 2018. Spawning aggregations act as a bottleneck influencing climate change impacts on a critically endangered reef fish. *Diversity and Distributions*, 24: 1712–1728.

Barbeaux, S. J., and Hollowed, A. B. 2018. Ontogeny matters: climate variability and effects on fish distribution in the eastern Bering Sea. *Fisheries Oceanography*, 27: 1–15.

Bennie, J., Hodgson, J. A., Lawson, C. R., Holloway, C. T. R., Roy, D. B., Brereton, T., Thomas, C. D., *et al.* 2013. Range expansion through fragmented landscapes under a variable climate. *Ecology Letters*, 16: 921–929.

, 2016. Interactive effects of incubation temperature and salinity on the early life stages of pacific cod *Gadus macrocephalus*. *Deep Sea Research Part II: Topical Studies in Oceanography*, 124: 117–128.

Bian, X., Zhang, X., Sakurai, Y., Jin, X., Gao, T., Wan, R., and Yamamoto, J. 2014. Temperature-mediated survival, development and hatching variation of Pacific cod *Gadus macrocephalus* eggs. *Journal of Fish Biology*, 84: 85–105.

Burrows, M. T., Schoeman, D. S., Richardson, A. J., Molinos, J. G., Hoffmann, A., Buckley, L. B., Moore, P. J., *et al.* 2014. Geographical lim-

its to species-range shifts are suggested by climate velocity. *Nature*, 507: 492–495.

Cheng, W., Hermann, A. J., Hollowed, A. B., Holsman, K. K., Kearney, K. A., Pilcher, D. J., Stock, C. A., *et al.* 2021. Eastern Bering Sea shelf environmental and lower trophic level responses to climate forcing: results of dynamical downscaling from CMIP6. *Deep Sea Research Part II: Topical Studies in Oceanography*, 193: 104975.

Cheung, W. W. L., Sarmiento, J. L., Dunne, J., Frölicher, T. L., Lam, V. W. Y., Deng Palomares, M. L., Watson, R., *et al.* 2013. Shrinking of fishes exacerbates impacts of global ocean changes on marine ecosystems. *Nature Climate Change*, 3: 254–258.

Ciannelli, L., Bailey, K., and Olsen, E. M. 2015. Evolutionary and ecological constraints of fish spawning habitats. *ICES Journal of Marine Science*, 72: 285–296.

Ciannelli, L., Neuheimer, A. B., Stige, L. C., Frank, K. T., Durant, J. M., Hunsicker, M., Rogers, L. A., *et al.* 2021. Ontogenetic spatial constraints of sub-arctic marine fish species. *Fish and Fisheries*, 23: 342–357.

Coachman, L. K. 1986. Circulation, water masses, and fluxes on the southeastern Bering Sea shelf. *Continental Shelf Research*, 5: 23–108.

Cote, D., Konecny, C. A., Seiden, J., Hauser, T., Kristiansen, T., and Laurel, B. J. 2021. Forecasted Shifts in Thermal Habitat for Cod Species in the Northwest Atlantic and Eastern Canadian Arctic. *Frontiers in Marine Science*, 8: 764072.

Coulson, M. W., Marshall, H. D., Pepin, P., and Carr, S. M. (2006). Mitochondrial genomics of gadine fishes: implications for taxonomy and biogeographic origins from whole-genome data sets. *Genome*, 49(9): 1115–1130.

Dahlke, F. T., Butzin, M., Nahrgang, J., Puvanendran, V., Mortensen, A., Pörtner, H.-O., and Storch, D. 2018. Northern cod species face spawning habitat losses if global warming exceeds 1.5°C. *Science Advances*, 4: eaas8821.

Dahlke, F. T., Wohlrab, S., Butzin, M., and Pörtner, H.-O. 2020. Thermal bottlenecks in the life cycle define climate vulnerability of fish. *Science*, 369: 65–70.

Deutsch, C., Penn, J. L., and Seibel, B. 2020. Metabolic trait diversity shapes marine biogeography. *Nature*, 585: 557–562.

Dodson, J. J., Daigle, G., Hammer, C., Polte, P., Kotterba, P., Winkler, G., and Zimmermann, C. 2019. Environmental determinants of larval herring (*Clupea harengus*) abundance and distribution in the western Baltic Sea. *Limnology and Oceanography*, 64: 317–329.

Dulvy, N. K., Rogers, S. I., Jennings, S., Stelzenmller, V., Dye, S. R., and Skjoldal, H. R. 2008. Climate change and deepening of the North Sea fish assemblage: a biotic indicator of warming seas. *Journal of Applied Ecology*, 45: 1029–1039.

Evans, T. G., Diamond, S. E., and Kelly, M. W. 2015. Mechanistic species distribution modelling as a link between physiology and conservation. *Conservation Physiology*, 3:cov056.

Farley, E. V., Heintz, R. A., Andrews, A. G., and Hurst, T. P. 2016. Size, diet, and condition of age-0 Pacific cod (*Gadus macrocephalus*) during warm and cool climate states in the eastern Bering Sea. *Deep Sea Research Part II: Topical Studies in Oceanography*, 134: 247–254.

Fissel, B., Dalton, M., Garber-Yonts, B., Haynie, A. C., Kasperski, S., Lee, Jean, Lew, D., *et al.* 2019. Stock Assessment and Fishery Evaluation Report for the groundfish fisheries of the Gulf of Alaska and Bering Sea/Aleutian Islands Area: economic Status of the Groundfish Fisheries Off Alaska, 2018. Groundfish SAFE Economic Report. 385pp.

Fossheim, M., Primicerio, R., Johannessen, E., Ingvaldsen, R. B., Aschan, M. M., and Dolgov, A. V. 2015. Recent warming leads to a rapid borealization of fish communities in the Arctic. *Nature Climate Change*, 5: 673–677.

Fredston, A., Pinsky, M., Selden, R. L., Szuwalski, C., Thorson, J. T., Gaines, S. D., and Halpern, B. S. 2021. Range edges of North American marine species are tracking temperature over decades. *Global Change Biology*, 27: 3145–3156.

Hawkins, E., Osborne, T. M., Ho, C. K., and Challinor, A. J. 2013. Calibration and bias correction of climate projections for crop mod-elling: an idealised case study over Europe. *Agricultural and Forest Meteorology*, 170: 19–31.

Hayes, D. B., Ferreri, C. P., and Taylor, W. W. 1996. Linking fish habitat to their population dynamics. *Canadian Journal of Fisheries and Aquatic Sciences*, 53: 383–390.

Haynie, A. C., and Pfeiffer, L. 2013. Climatic and economic drivers of the Bering Sea walleye pollock (*Theragra chalcogramma*) fishery: implications for the future. *Canadian Journal of Fisheries and Aquatic Sciences*, 70: 841–853.

Hermann, A. J., Kearney, K., Cheng, W., Pilcher, D., Aydin, K., Holsman, K. K., and Hollowed, A. B. 2021. Coupled modes of projected regional change in the Bering Sea from a dynamically downscaling model under CMIP6 forcing. *Deep Sea Research Part II: Topical Studies in Oceanography*, 194: 104974.

Hollowed, A. B., Hare, S. R., and Wooster, W. S. 2001. Pacific Basin climate variability and patterns of Northeast Pacific marine fish production. *Progress in Oceanography*, 49: 257–282.

Holsman, K. K., Haynie, A. C., Hollowed, A. B., Reum, J. C. P., Aydin, K., Hermann, A. J., Cheng, W., *et al.* 2020. Ecosystem-based fisheries management forestalls climate-driven collapse. *Nature Communications*, 11: 4579.

Houde, E. D. 2008. Emerging from Hjort's Shadow. *Journal of Northwest Atlantic Fishery Science*, 41: 53–70.

Kearney, K., Hermann, A., Cheng, W., Ortiz, I., and Aydin, K. 2020. A coupled pelagic–benthic–sympagic biogeochemical model for the Bering Sea: documentation and validation of the BESTNPZ model (v2019.08.23) within a high-resolution regional ocean model. *Geoscientific Model Development*, 13: 597–650.

Kleisner, K. M., Fogarty, M. J., McGee, S., Hare, J. A., Moret, S., Perretti, C. T., and Saba, V. S. 2017. Marine species distribution shifts on the U.S. Northeast Continental Shelf under continued ocean warming. *Progress in Oceanography*, 153: 24–36.

Laman, E. A., Pirtle, J. L., Harris, J., Siple, M. C. Rooper, C. N. Hurst, T. P., and Conrath, C. L. 2022. Advancing model-based essential fish habitat descriptions for North Pacific species in the Bering Sea. NOAA technical memorandum NMFS-AFSC; 459. <https://doi.org/10.25923/y5gc-nk42>

Laurel, B. J., Hunsicker, M. E., Ciannelli, L., Hurst, T. P., Duffy-Anderson, J., O'Malley, R., and Behrenfeld, M. 2021. Regional warming exacerbates match/mismatch vulnerability for cod larvae in Alaska. *Progress in Oceanography*, 193: 102555.

Laurel, B. J., Hurst, T. P., Copeman, L. A., and Davis, M. W. 2008. The role of temperature on the growth and survival of early and late hatching Pacific cod larvae (*Gadus macrocephalus*). *Journal of Plankton Research*, 30: 1051–1060.

Laurel, B. J., and Rogers, L. A. 2020. Loss of spawning habitat and pre-recruits of Pacific cod during a Gulf of Alaska heatwave. *Canadian Journal of Fisheries and Aquatic Sciences*, 77: 644–650.

Matarese, A. C., Blood, D. M., Picquelle, S. J., and Benson, J. L. 2003. *Atlas of Abundance and Distribution Patterns of Ichthyoplankton from the Northeast Pacific Ocean and Bering Sea Ecosystems Based on Research Conducted by the Alaska Fisheries Science Center (1972–1996)*. NOAA Professional Paper NMFS 1.

Mizobata, K., Wang, J., and Saitoh, S. 2006. Eddy-induced cross-slope exchange maintaining summer high productivity of the Bering Sea shelf break. *Journal of Geophysical Research*, 111: C10017.

Morley, J. W., Selden, R. L., Latour, R. J., Frölicher, T. L., Seagraves, R. J., and Pinsky, M. L. 2018. Projecting shifts in thermal habitat for 686 species on the North American continental shelf. *PLoS ONE*, 13:e0196127.

Mueter, F. J., and Litzow, M. A. (2008). Sea ice retreat alters the biogeography of the Bering Sea continental shelf. *Ecological Applications*, 18: 309–320.

Munday, P. L., Jones, G. P., Pratchett, M. S., and Williams, A. J. 2008. Climate change and the future for coral reef fishes. *Fish and Fisheries*, 9: 261–285.

Neidetcher, S. K., Hurst, T. P., Ciannelli, L., and Logerwell, E. A. 2014. Spawning phenology and geography of Aleutian Islands and eastern

Bering Sea Pacific cod (*Gadus macrocephalus*). Deep Sea Research Part II: Topical Studies in Oceanography, 109: 204–214.

O'Neill, B. C., Tebaldi, C., van Vuuren, D. P., Eyring, V., Friedlingstein, P., Hurtt, G., Knutti, R., et al. 2016. The scenario model intercomparison project (ScenarioMIP) for CMIP6. Geoscientific Model Development, 9: 3461–3482.

Parmesan, C., and Yohe, G. 2003. A globally coherent fingerprint of climate change impacts across natural systems. *Nature*, 421: 37–42.

Pinsky, M. L., and Fogarty, M. 2012. Lagged social-ecological responses to climate and range shifts in fisheries. *Climatic Change*, 115: 883–891.

Pinsky, M. L., Rogers, L. A., Morley, J. W., and Frölicher, T. L. 2020. Ocean planning for species on the move provides substantial benefits and requires few trade-offs. *Science Advances*, 6. <https://doi.org/10.1126/sciadv.abb8428>

Pinsky, M. L., Worm, B., Fogarty, M. J., Sarmiento, J. L., and Levin, S. A. 2013. Marine taxa track local climate velocities. *Science*, 341: 1239–1242.

Poloczanska, E. S., Brown, C. J., Sydeman, W. J., Kiessling, W., Schaeffer, D. S., Moore, P. J., Brander, K., et al. 2013. Global imprint of climate change on marine life. *Nature Climate Change*, 3: 919–925.

Pörtner, H. O., and Farrell, A. P. 2008. Physiology and Climate Change. *Science*, 322: 690–692.

Pörtner, H.-O. 2021. Climate impacts on organisms, ecosystems and human societies: integrating OCLTT into a wider context. *Journal of Experimental Biology*, 224: jeb238360.

Rand, K. M., Munro, P., Neidetcher, S. K., and Nichol, D. G. 2014. Observations of seasonal movement from a single tag release group of Pacific cod in the eastern Bering Sea. *Marine and Coastal Fisheries*, 6: 287–296.

Rijnsdorp, A. D., Peck, M. A., Engelhard, G. H., Möllmann, C., and Pinnegar, J. K. 2009. Resolving the effect of climate change on fish populations. *ICES Journal of Marine Science*, 66: 1570–1583.

Rogers, L. A., and Dougherty, A. B. 2019. Effects of climate and demography on reproductive phenology of a harvested marine fish population. *Global Change Biology*, 25: 708–720.

Rogers, L. A., Griffin, R., Young, T., Fuller, E., Martin St., K., and Pinsky, M. L. 2019. Shifting habitats expose fishing communities to risk under climate change. *Nature Climate Change*, 9: 512–516.

Rogers, L. A., Wilson, M. T., Duffy-Anderson, J. T., Kimmel, D. G., and Lamb, J. F. 2021. Pollock and “the Blob”: impacts of a marine heatwave on walleye pollock early life stages. *Fisheries Oceanography*, 30: 142–158.

Saha, S., Moorthi, S., Pan, H. L., Wu, X., Wang, J., Nadiga, S., Tripp, P., et al. 2010. The NCEP climate forecastsystem reanalysis. *B. Am. Meteorol. Soc.*, 91: 1015–1057.

Sigler, M. F., Harvey, H. R., Ashjian, J., Lomas, M. W., Napp, J. M., Stabeno, P. J., and Van Pelt, T. I. 2010. How does climate change affect the Bering Sea ecosystem? *Eos, Transactions American Geophysical Union*, 91: 457.

Stabeno, P. J., and Bell, S. W. 2019. Extreme conditions in the Bering Sea (2017–2018): record-breaking low sea-ice extent. *Geophysical Research Letters*, 46: 8952–8959.

Stabeno, P. J., Kachel, N. B., Moore, S. E., Napp, J. M., Sigler, M., Yamaguchi, A., and Zerbini, A. N. 2012. Comparison of warm and cold years on the southeastern Bering Sea shelf and some implications for the ecosystem. *Deep Sea Research Part II: Topical Studies in Oceanography*, 65–70: 31–45.

Stevenson, D. E., and Lauth, R. R. 2019. Bottom trawl surveys in the northern Bering Sea indicate recent shifts in the distribution of marine species. *Polar Biology*, 42: 407–421.

Sumaila, U. R., Cheung, W. W. L., Lam, V. W. Y., Pauly, D., and Herrick, S. 2011. Climate change impacts on the biophysics and economics of world fisheries. *Nature Climate Change*, 1: 449–456.

Sunday, J., Bennett, J. M., Calosi, P., Clusella-Trullas, S., Gravel, S., Hargreaves, A. L., Leiva, F. P., et al. 2019. Thermal tolerance patterns across latitude and elevation. *Philosophical Transactions of the Royal Society B: Biological Sciences*, 374: 20190036.

Thompson, G. G., Barbeaux, S., Conner, J., Fissel, B., Hurst, T., Laurel, B., O’Leary, C. A., et al. 2021. Assessment of the Pacific Cod Stock in the Eastern Bering Sea. 494.

Tsoukali, S., Visser, A., and MacKenzie, B. 2016. Functional responses of North Atlantic fish eggs to increasing temperature. *Marine Ecology Progress Series*, 555: 151–165.

Watson, J. T., and Haynie, A. C. 2018. Paths to resilience: the walleye pollock fleet uses multiple fishing strategies to buffer against environmental change in the Bering Sea. *Canadian Journal of Fisheries and Aquatic Sciences*, 75: 1977–1989.

Zhang, J. 2005. Warming of the arctic ice-ocean system is faster than the global average since the 1960s: faster warming arctic ice-ocean system. *Geophysical Research Letters*, 32: L19602.

Handling editor: Manuel Hidalgo